ScienceDirect

IFAC PapersOnline CONFERENCE PAPER ARCHIVE

IFAC PapersOnLine 51-2 (2018) 837–842

A vehicle model for crash stage simulation

Dario Vangi*, Filippo Begani*, Michelangelo-Santo Gulino*
Florian Spitzhüttl**

** Department of Industrial Engineering, University of Florence, 50139 Florence, Italy, (e-mail: michelangelo.gulino@unifi.it)*
***Institute for Traffic Accident Research at Dresden University of Technology (VUFO), 01069 Dresden, Germany, (e-mail:florian.spitzhuettl@vufo.de)*

Abstract: Simulation of vehicle impact stages is gaining more importance as the years go by. The reasons are an increase in the requested vehicles performances in terms of passive and active safety but also the necessity to investigate causes which lead to car accidents. The paper describes a special purpose 2D vehicle model for time-efficient crash stage simulation and therefore introduces the equations which rule over the model first. The Finite Element Method (FEM) represents the basis for the analytical formulation of the problem. However, the different stiffness of the various vehicle areas involves a calibration of the model, using real vehicle-to-barrier crash tests as a reference (carried out by EuroNCAP, NHTSA, etc.). Based on the obtained stiffness value, performed simulations demonstrate the applicability of the method to real vehicle-to-vehicle impacts contained in databases like AREC, VERSUE, etc. Furthermore, real-world crashes and results of the developed model simulations are compared for four different exemplary cases, highlighting the possibility to fully describe the events dynamics and the vehicles deformations. Therefore, the described model simulation times are evidently shortened in respect to more complicated solution approaches, like FEM or Multi-Body models. These resources savings also imply the possibility to simulate activation of Advanced Driving Assistance Systems (ADAS), i.e. the simulation of multiple impact configurations as the ADAS features vary.

Keywords: Crash simulation, Reduced order models, Numerical simulation, Traffic accidents

1. INTRODUCTION

Vehicles impact behaviour has always been an attractive topic in the research field. The knowledge about structural response to crashes for various means of transport can be decisive in many different applications. The most advanced techniques to simulate crashes allow for the structural optimization of vehicles (crashworthiness) to enhance occupants' safety, as well as for the reconstruction of road accidents dynamics. In the last few years, simulation algorithms also permitted the enhancement or optimization of specific Advanced Driver Assistance Systems (ADAS) features (Ming, et al., 2016) which actively change pre-crash conditions of the vehicles. Because of these enhancements which involve many types of road users, from 2010 to 2015 the number of road fatalities in the European Union (EU) decreased of about 17 % (European Road Safety Observatory, 2017). Nevertheless, still 3 people die each hour, requiring steps forward also in the simulative approaches, to achieve near-zero fatalities in 2050 as prescribed by the EU Transport White Paper. These enhancements also result in the need to generate more synthetic data to evaluate ADAS performances, leading to a significant increase in the number of simulation runs with different crash configurations. Considering the complexity of existing simulation methods, this raises the necessity to reduce computation times significantly.

Currently a wide range of numerical methods is in use for crash dynamics evaluation purposes (Brach & Brach, 2005):

1. Finite Element Models (FEM) requiring the vehicle to be discretized in a very large number of elements. Because of the high deformations and displacements implied in the crash, the ruling equations are constituted of many non-linear terms and the approach is referred to as Non-Linear FEM (Pawlus, et al., 2011). The method is accurate, but the calculation times are high, so the method is generally employed in the last part of a new vehicle design phase, when the few vehicle models available in libraries are analysed (Yildiz & Solanki, 2012) or to investigate crashworthiness features of particular components (Wei, et al., 2016). Examples for commercial FEM software are LS-DYNA©, ABAQUS© or ANSYS©.
2. Multi-body (MB) models, in which different portions of the vehicle are connected through kinematic joints. Forces are exchanged by those constraints: the parts are rigid and the shape variation depends on relative movements. However, Addition of FEM can be used to consider single parts deformations (Hamza & Saitou, 2005). The Lagrange method is the most applied in this type of analysis, based on the D'Alembert's principle. MB methods generally allow to analyse models' kinematics and, regarding vehicle crashes, to solve crash dynamics quicker than in the FEM case; it is commonly used in the early design stages of a vehicle, to study crashworthiness features, or for accident reconstruction purposes. Some software examples are MADYMO© (TASS Int.), SIMPACK© and MUSIAC©.
3. Impulsive models, based on momentum conservation and determining deformation energy and velocities of the vehicles after the impact starting from the initial conditions (forward reconstruction) or vice versa (backward reconstruction). This

10.1016/j.ifacol.2018.04.018

method is widely used because of the low calculation times, but it does not provide any information about vehicles' deformations nor accelerations (Brach, 1983; Ishikawa, 1993; Kolk, et al., 2016). PC-Crash©, Virtual Crash©, etc. are software packages which mainly use impulsive models.

4. Response Surface Models (RSM), appropriate for crashworthiness analysis (Simpson, et al., 2004). The vehicle impact behaviour is determined making use of a testing campaign: first, a full factorial Design Of Experiment (DOE) is created to consider all intended parameters, then data are acquired (from real tests or simulations) and eventually fitted to generate an analytical formulation describing the vehicle behaviour. The vehicle features are thus reconstructed making use of calculations, but no special purpose software is available to automate the process.

5. Reduced Order Dynamic Models (RODM) which are mainly based on FEM methods, with approximations of the problem to solve it more quickly. These methods have a lower accuracy in respect to the FEM. The most used category of RODM is the lumped-mass model (Jonsén, et al., 2009; Pahlavani & Marzbanrad, 2015) that substitute masses, dampers and springs to structural elements.

While pure MB models (with rigid body) can accurately simulate the driving dynamics, no deformation is calculated. FEM and RSM model approaches calculate the deformations but provides for insufficient vehicle dynamics output. The paper thus describes a RODM routine providing both deformed shapes of vehicles and thorough information regarding accident kinematics and dynamics, as respectively obtainable from FEM/RSM and MB/impulsive model simulations.

Road accidents can also be simulated trying out different impact configurations in a short time and can be combined with impulse models to get more detailed information on deformations and post-impact velocities and directions. Lower simulation time (ensuring a good accuracy) is a particularly desirable feature in all engineering problems because costs are reduced; this feature can be also decisive in ADAS control logic design: in real road conditions, the ADAS intervention minimizing damages to vehicles and occupants can be outlined almost in real time. The algorithm consists in a lumped-mass model, in which the vehicle discretization affects only its perimeter. The vehicle is treated in 2D, making the model suitable for crash analysis and reconstruction. The vehicle model considers only rods with little possibility to extend or shorten and that do not transmit bending moments. Rods are without mass and linked together by nodes as in the FEM. Deformation of the vehicle as a whole is the result of nodes displacements only, caused by the impact. Forces are transferred to nodes by springs, linked to nodes at one end and to a virtual point on the vehicle at the other end, coinciding with nodal position before vehicle's deformation (called non-deformed virtual vehicle). For the integration of motion equations, the inertial properties of the vehicle are applied on the centre of gravity. Elastic properties of springs can be determined from load-deformation curves slope obtained from crash tests or FEM simulations (McHenry, 1997). PC-Crash simulations will be used as reference to evaluate the proposed RODM performances in real-road accidents reconstruction.

2. MODEL DEVELOPMENT

Figure 1 shows two standard vehicle models penetrating each other due to an impact. The RODM algorithm discretizes only the perimeter of the vehicle or infrastructural element, at the height of the platform. The vehicle models' perimeters are divided in 50 elements each which are sufficient to describe, in a satisfactory manner, their crash behaviour for accident reconstruction purposes. The elements transmit only tensile or compressive forces, and no bending state is allowed. The elements have only little possibility of changing their lengths in a predefined limit, to increase the solver calculation efficiency. The simulation starts at the impact instant.

During the simulated impact and at each time step (some millisecond long), contact between the two vehicles' surface is detected by means of an algorithm determining which nodes of vehicle A are positioned inside vehicle B and vice versa. The vehicles are initially moved in the direction of initial speed v_i. Forces between the vehicles' nodes are assumed to act in the direction of relative motion, also referred to as PDOF (Vangi, 2008; Vangi, 2009), at the considered time step; such direction is obtained through the vector difference between the vehicles velocity. First attempt forces are imposed on each node; considering pairs of nodes, belonging to different vehicles, which are closest along the PDOF, iteration is repeated until the sum of their displacements reaches the distance at the time step beginning. Inertial properties of the vehicles are neglected and applied once the calculation is completed, to re-evaluate the vehicle's velocity and displacements at the subsequent time-step. The process is then applied identically at the following time-step as long as an intrusion area exists.

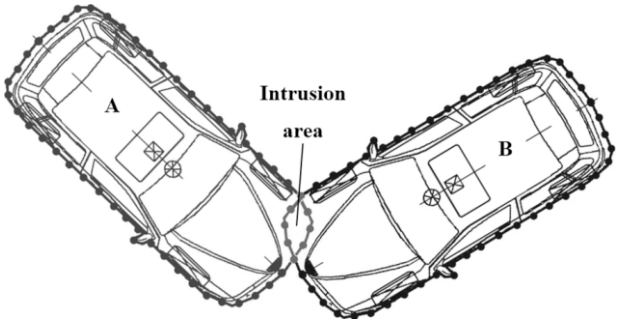

Fig. 1. Two impacting vehicles with intruded nodes (light grey) and perimeters discretization in 50 elements each.

To better understand the proposed method, figure 2 shows a *n* nodes simplified model: the rods lie on a straight line and the problem is in 1D. Nodes are connected to the non-deformable virtual vehicle by transversal *x* and longitudinal *y* springs applied on nodes. Springs follow Campbell model (Campbell, 1974), i.e. the vehicle is assumed to act as a homogeneous mean and to have a macroscopic linear behaviour. Springs stiffness varies from point to point, with different values in correspondence of side, front, corner and wheel nodes.

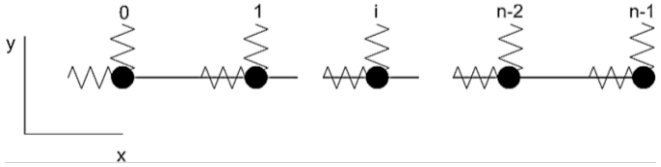

Fig. 2. 1D representation of a vehicle's perimeter, with the nodes linked by springs to the virtual vehicle.

Vehicles' motion is described by integrating motion equations in a single time step, also considering the forces transmitted by the wheels to the road; the latter are computed by the classical adherence circle model, like the one used in PC-Crash.

By indicating with $T_{(i\_i+1)}$ the forces transmitted through the rod linking nodes *i* and *i+1*, with k_i the elastic constant of the springs relative to node *i*, with x_i and y_i node *i* coordinates, with x_i^0 and y_i^0 its coordinates at the time step beginning (non-deformed vehicle) and with F_j the force applied to node j, the following equations (Eq. 1-4) for n nodes can be written:

Equilibrium equations along the x axis (*n* equations)

$$
\begin{aligned}
&k_{0x}(x_0 - x_0^0) - T_{(0_1)x} = 0\\
&k_{1x}(x_1 - x_1^0) + T_{(0\_1)x} - T_{(1\_2)x} = 0\\
&\dots\dots\dots\dots\dots\dots\\
&k_{(i)x}(x_i - x_i^0) + T_{(i-1\_i)x} - T_{(i\_i+1)x} = 0\\
&\dots\dots\dots\dots\dots\dots\\
&k_{jx}\left(x_j - x_j^0\right) + T_{(j-1\_j)x} - T_{(j\_j+1)x} + F_{jx} = 0\\
&\dots\dots\dots\dots\dots\dots\\
&k_{(n-2)x}(x_{n-2} - x_{n-2}^0) + T_{(n-3\_n-2)y} - T_{(n-2\_n-1)x} = 0\\
&k_{(n-1)x}(x_{n-1} - x_{n-1}^0) + T_{(n-2\_n-1)x} = 0
\end{aligned}
\tag{1}
$$

Equilibrium equations along the y axis (*n* equations)

$$
\begin{aligned}
&k_{0y}(y_0 - y_0^0) - T_{(0\_1)y} = 0\\
&k_{1y}(y_1 - y_1^0) + T_{(0\_1)y} - T_{(1\_2)y} = 0\\
&\dots\dots\dots\dots\dots\dots\\
&k_{(i)y}(y_i - y_i^0) + T_{(i-1\_i)y} - T_{(i\_i+1)y} = 0\\
&\dots\dots\dots\dots\dots\dots\\
&k_{jy}\left(y_j - y_j^0\right) + T_{(j-1\_j)y} - T_{(j\_j+1)y} + F_{jy} = 0\\
&\dots\dots\dots\dots\dots\dots\\
&k_{(n-2)y}(y_{n-2} - y_{n-2}^0) + T_{(n-3\_n-2)y} - T_{(n-2\_n-1)y} = 0\\
&k_{(n-1)y}(y_{n-1} - y_{n-1}^0) + T_{(n-2\_n-1)y} = 0
\end{aligned}
\tag{2}
$$

Constancy of distance d_i between consecutive nodes within a certain tolerance ε (*n-1* equations)

$$
\begin{aligned}
&(x_1 - x_0)^2 + (y_1 - y_0)^2 < (d_0 + \varepsilon)^2\\
&(x_2 - x_1)^2 + (y_2 - y_1)^2 < (d_1 + \varepsilon)^2\\
&\dots\dots\dots\dots\dots\dots\\
&(x_i - x_{i-1})^2 + (y_i - y_{i-1})^2 < (d_{i-1} + \varepsilon)^2\\
&\dots\dots\dots\dots\dots\dots\\
&\left(x_j - x_{j-1}\right)^2 + \left(y_j - y_{j-1}\right)^2 < \left(d_{j-1} + \varepsilon\right)^2\\
&\dots\dots\dots\dots\dots\dots\\
&(x_{n-2} - x_{n-3})^2 + (y_{n-2} - y_{n-3})^2 < (d_{n-3} + \varepsilon)^2\\
&(x_{n-1} - x_{n-2})^2 + (y_{n-1} - y_{n-2})^2 < (d_{n-2} + \varepsilon)^2
\end{aligned}
\tag{3}
$$

T_{i_j} rod internal forces aligned with the axis of the element itself (*n-1* equations)

$$
\begin{aligned}
&\frac{T_{(0\_1)x}}{T_{(0\_1)y}} = \frac{x_1 - x_0}{y_1 - y_0}\\
&\frac{T_{(1\_2)x}}{T_{(1\_2)y}} = \frac{x_2 - x_1}{y_2 - y_1}\\
&\dots\dots\dots\dots\dots\dots\\
&\frac{T_{(i-1\_i)x}}{T_{(i-1\_i)y}} = \frac{x_i - x_{i-1}}{y_i - y_{i-1}}\\
&\dots\dots\dots\dots\dots\dots\\
&\frac{T_{(j-1\_j)x}}{T_{(j-1\_j)y}} = \frac{x_j - x_{j-1}}{y_j - y_{j-1}}\\
&\dots\dots\dots\dots\dots\dots\\
&\frac{T_{(n-3\_n-2)x}}{T_{(n-3\_n-2)y}} = \frac{x_{n-2} - x_{n-3}}{y_{n-2} - y_{n-3}}\\
&\frac{T_{(n-2\_n-1)x}}{T_{(n-2\_n-1)y}} = \frac{x_{n-1} - x_{n-2}}{y_{n-1} - y_{n-2}}
\end{aligned}
\tag{4}
$$

The unknowns are the x and y nodal coordinates (*2n*) and the T_{i_j} forces components (*2n-2*), resulting in a total amount of *4n-2* equations in *4n-2* unknowns. The equations are not linear and must be solved with numerical methods or algorithms like the Newton's or quasi-Newton (e.g. Newton-Raphson's) ones.

Once the displacements and tensions are obtained for both the vehicles, a check is performed to determine if the sum of the displacements is equal (within a certain tolerance) to the intrusion. If so, the force calculation process ends and the equations of motion are applied to the vehicles. If not, the first attempt forces values are changed based on how much the displacement of the related node is close to the intrusion. The algorithm is iterative, making it necessary to change first attempt forces and iterate until the criterion is fulfilled.

When the direction of vehicles' superimposition inverts, the restitution phase occurs (McHenry, 1997; Goldsmith, 2001) and different elastic constants *k* are applied, according to the desired load-crush law of the vehicle. When contact forces become null, the collision stage ends and the vehicles enter a post-collision phase, in which only road-tire forces are present.

The springs' elastic constants are determined by comparing the vehicles deformation to the ones obtained in real crash tests. Assuming the system is linear (Campbell model), a linear relation also exists between stiffness of different vehicle's areas. The characterization of the front area through a comparison with vehicle-to-barrier crash tests allows thus for the stiffness evaluation of all the vehicle's different areas.

More than 3000 vehicle-to-barrier crash tests have been analysed considering EuroNCAP, NHTSA and LaSIS (University of Florence) databases: the resulting stiffness allows to obtain the best-fitting post-impact motion, deformed shapes, pre-impact and post-impact velocities in respect to the real ones. Interestingly, the stiffness evaluation carried out in this study seems to point out that this parameter is peculiar to each class of vehicles (sedans, small cars, SUVs, etc.).

The possibility to efficiently simulate vehicle-to-barrier impacts is not sufficient by itself, because they represent a low amount of real-world cases. So, the ability to appropriately reconstruct vehicle-to-vehicle impacts through the RODM has been investigated, recreating crash tests gathered inside databases like AREC and VERSUE. The coherent results obtained imply only the necessity to further validate the model by comparison with real accidents data.

3. REAL CASES FOR MODEL VALIDATION

PC-Crash impulsive model simulations results are considered efficient indicators of the real accident kinematics: the comparison with the proposed RODM is based mainly on the Δv, representing the vector difference between the vehicles collision velocities v_i and post-impact velocities v_f; also, the Equivalent Energy Speed (EES) is reported, because it helps in reducing the analysed crash to a barrier impact, simpler to treat and to visualize (Vangi, 2008). On the other hand, the vehicles' deformed shapes obtained through the presented RODM are compared to pictures shot at the accident site: in fact, PC-Crash does not implement deformed shapes calculation.

The reconstruction of 4 real road accidents included in the German In-Depth Accident Study (GIDAS) database are analysed in detail, to highlight the suitability of the proposed method for the solution of practical problems. In each of these cases, the areas interested by the impact are mostly the ones with different stiffness in a vehicle (front, rear, side, wheel). Numerical results of simulations are reported in Chapter 4, addressing also simulation times.

3.1 Rear-end impact

Figure 4 shows a rear-end impact involving a FIAT Fiorino and an Audi A4 in an accident along a straight, one-way road before an intersection. The maximum intrusion condition is highlighted in light grey, while the final positions in dark grey (no intrusion). The Audi A4 was still, while the estimated impact speed v_i of the FIAT Fiorino was 25 km/h.

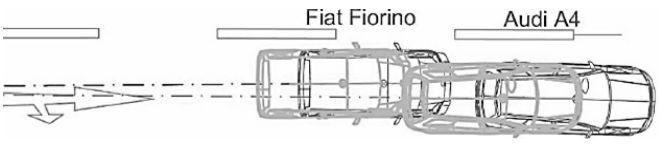

Fig. 4. Rear-end collision site with maximum intrusion condition (light grey) and final (dark grey) positions of the involved vehicles.

3.2 Frontal impact

Figure 5 shows the planimetry regarding the site of a frontal impact between a Toyota Corolla and a Chevrolet Kalos. The area of the road where the two vehicles collided is indicated by the presence of debris and depicted as a circle.

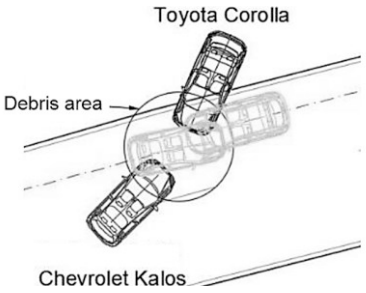

Fig. 5. Frontal impact with maximum intrusion (light grey) and final (dark grey) positions of the involved vehicles.

3.3 Side impact

In the intersection-located side impact shown in Figure 6, a Skoda Fabia and a BMW 550I were involved.

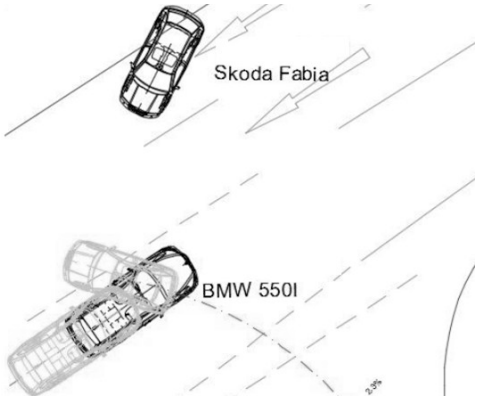

Fig. 6. Side impact site with maximum intrusion condition (light grey) and final (dark grey) positions of the involved vehicles.

3.4 Wheel engagement / Small overlap

Figure 7 shows an accident where a wheel engagement and small overlap crash between two vehicles occurred. A Toyota Avensis hit a Renault Master and then a Mercedes A-Class as a result of the first crash. The Mercedes was considered for the determination of the Toyota rest position only.

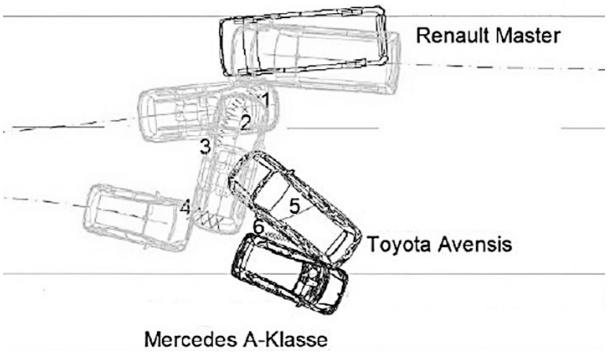

Fig. 7. Accident site for a small overlap crash: maximum intrusion condition (light grey) and final (dark grey) positions are reported.

4. RESULTS AND DISCUSSION

Comparing data between PC-Crash and the proposed RODM simulations summarized in Table 1 for the analysed impact scenarios, a high similarity in results can be assessed for what regards the post-impact velocity v_f and the speed change Δv. In fact, the maximum calculated difference is about 3 km/h which cannot generate evident consequences on the real road accident dynamics. Only the very rare and special impact constellation of the small overlap crash presents a significant difference of the parameters. This is due to the special wheel engagement and the involved front suspension. Δv represents the main parameter to be considered because it is an index of both vehicles deformations (Iraeus & Lindquist, 2015) and injury risk for the occupants (Ranfagni, et al., 2017). On the other hand, the EES calculated values are slightly different (reaching more than 10 km/h) based on the used algorithm; while these differences are important, it is also worth noting that the EES is based on the dissipated deformation energy. If the deformations are available as in the RODM case, the check is carried out comparing the calculated to the real ones rather than considering the EES.

Deformed shapes of the vehicles are shown in Figures 8-11, both calculated – (a) and (b) – and real ones – (c) and (d). The vehicles deformations obtained through the reconstruction correspond to the real ones with a high accuracy. This demonstrates the suitability of the proposed algorithm not only for accident reconstruction purposes, but also for crashworthiness assessment of vehicles in various impact configurations.

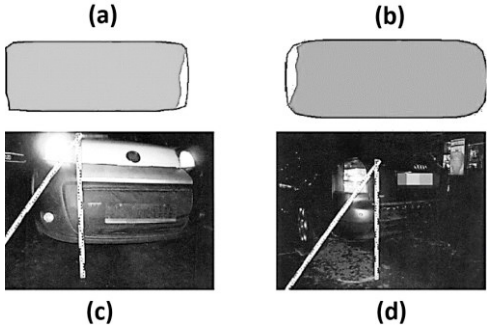

Fig. 8. Reconstructed deformed shapes of the Fiat Fiorino (a) and the Audi A4 (b) and the real ones (c,d).

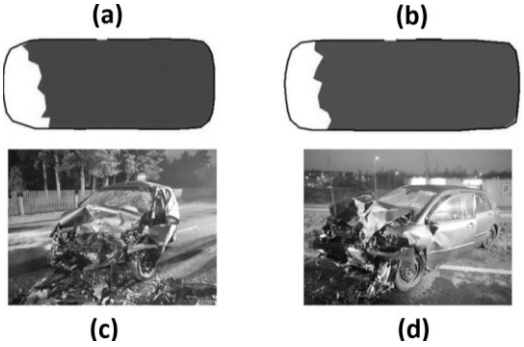

Fig. 9. Reconstructed deformed shapes of the Chevrolet Kalos (a) and the Toyota Corolla (b) and the real ones (c,d).

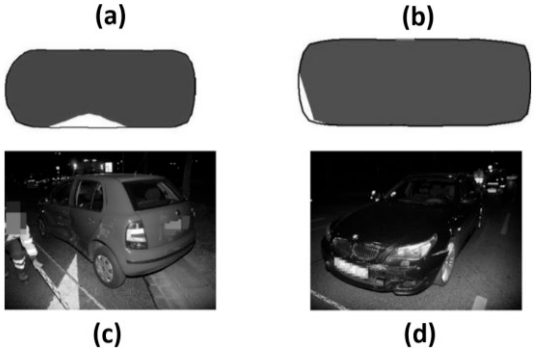

Fig. 10. Reconstructed deformed shapes of the Skoda Fabia (a) and the BMW 550I (b) and the real ones (c,d).

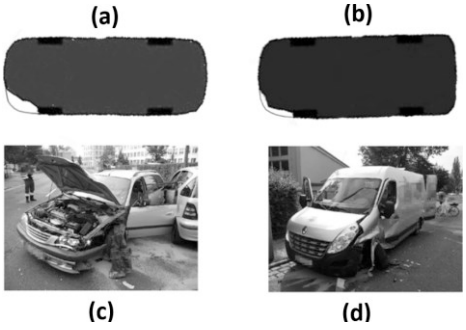

Fig. 11. Comparison between Toyota Avensis (a) and Renault Master (b) reconstructed deformed shapes with real ones (c,d).

Table 1. Initial conditions and results for the analysed scenario through PC-Crash and the proposed RODM.

Speed (km/h)	PC-Crash		RODM	
REAR-END	Fiorino	A4	Fiorino	A4
v_i	25	0	25	0
v_f	11	13	11	13
Δv	15	13	15	13
EES	12	12	12	12
FRONTAL	Kalos	Corolla	Kalos	Corolla
v_i	58	58	58	58
v_f	12	3	8	2
Δv	67	57	64	59
EES	59	54	47	65
SIDE	Fabia	550I	Fabia	550I
v_i	20	37	20	37
v_f	20	22	21	19
Δv	23	15	20	16
EES	24	19	18	25
WHEEL	Avensis	Master	Avensis	Master
v_i	40	30	40	30
v_f	9	11	10	13
Δv	41	26	31	20
EES	20	36	25	36

Simulation times (W7x64, Intel Xeon 3.5 GHz, 32GB RAM) for the analysed impacts t^s are:

1. Rear-end crash $t^s_{RE} = 7\ min$;
2. Frontal crash $t^s_F = 375\ min$;

3. Side crash $t_S^s = 15\ min$:
4. Wheel engagement $t_W^s = 32\ min$.

Calculation times for cases 1, 3 and 4 are extremely low in respect to traditional FEM and MB algorithms (of the order of days and hours respectively). This is less evident for case 2, in which they are comparable with the MB ones, probably due to high initial speeds and conditions superimposed for iterations. The accuracy is however the same for MB and RODM, making them interchangeable for this case reconstruction.

5. CONCLUSIONS

The present work introduced a special purpose Reduced Order Dynamic Model (RODM) for the vehicles crash stage simulation. The problem of long simulation times, deriving from Finite Elements Models (FEM) or Multi-Body (MB) approaches use, was addressed. Discretization of vehicle's perimeter only in a 2D environment reduces the number of analysed domains, simplifying equations to be solved inside them. The reconstruction accuracy can be assessed starting from a comparison between PC-Crash and the proposed RODM simulations regarding real road accidents. The RODM time for solution can be expressed in terms of minutes, while FEM and MB reconstruction times are of the order of days and hours respectively. 5 hours of RODM simulation were needed in the worst case, represented by a front impact at relatively high speed and involving high deformations. Time is however comparable to MB models' solution ones. The developed method proved to be an efficient alternative to every crash dynamics reconstruction commercial software. In fact, it can be used for multiple purposes in the road safety research field:

- road accidents reconstruction, for the investigation of their major causes;
- crashworthiness analysis, for the determination of vehicles dynamic response to crashes;
- ADAS simulations, for the study of new driving assistance systems and intervention verification in a specific event.

Valuable features of the described algorithm lie in the reduction of simulation times, in the accuracy of solution but also in the possibility to subsequently improve its efficiency. In fact, the RODM uses non-linear equations which involve iterative calculations; the next steps will be taken, starting from the algorithm described in this work, towards a linearity-based method capable of further reducing the simulation time.

REFERENCES

Brach, R. M., 1983. Analysis of Planar Vehicle Collisions Using Equations of Impulse and Momentum. Accident Analysis and Prevention, 15(2), pp. 105-120.

Brach, R. M. & Brach, M. R., 2005. Vehicle Accident Analysis and Reconstruction Methods. Warrendale, PA, USA: SAE International, ISBN 0-7680-0776-3.

Campbell, K., 1974. Energy as a Basis for Accident Severity. SAE Paper, Issue 740565.

European Road Safety Observatory, 2017. Annual Accident Report 2017.

European Commission, 2010. Road Safety Programme 2011-2020: detailed measures, European Commision.

GIDAS, 2017, http://gidas.org. [Online].

Goldsmith, W., 2001. Impact-The Theory and Physical Behaviour of Colliding Solids. Mineola, New York: Dover Publications, Inc..

Hamza, K. & Saitou, K., 2005. Design Optimization of Vehicle Structures for Crashworthiness Using Equivalent Mechanism Approximations. Transactions of ASME, Journal of Mechanical Design(127(3):), pp. 485-492.

Iraeus, J. & Lindquist, M., 2015. Pulse shape analysis and data reduction of real-life frontal crashes with modern passenger cars. Int. J. Crashworth., 20(6).

Ishikawa, H., 1993. Impact Model for Accident Reconstruction - Normal and Tangential Restitution Coefficients. SAE Paper, Issue 930654.

Jonsén, P., Isaksson, E., Sundin, K. & Oldenburg, M., 2009. Identifcation of lumped parameter automotive crash models for bumper system development. Int. J. Crashworth., 14(6), pp. 533-541.

Kolk, H. et al., 2016. Evaluation of a momentum based impact model and application in an effectivity study considering junction accidents. Hannover.

LSTC, n.d. www.lstc.com/products/ls-dyna. [Online].

M. Pahlavani, J. M., 2015. Crashworthiness study of a full vehicle- lumped model using parameters optimisation. Int. J. Crashworth., 20(6), pp. 573-591.

McHenry, R. a. M. B., 1997. Effects of Restitution in the Application of Crush Coefficients. SAE Technical Paper, Issue 970960.

Milano, P., http://hdl.handle.net/10589/51382. [Online].

Ming, L., Jaewoo, Y. & Byeongwoo, K., 2016. Proposal and Validation of AEB System Algorithm for Various Slope Environments. Advanced Multimedia and Ubiquitous Engineering, Lecture Notes in Electrical Engineering (354).

PC-Crash, 2017, www.pc-crash.it. [Online].

Pawlus, W., Karimi, H. R. & Robbersmyr, K. G., 2011. Application of viscoelastic hybrid models to vehicle crash simulation. Int. J. Crashworth., 16(2), pp. 195-205.

Ranfagni, S., Vangi, D. & Fiorentino, A., 2017. Road Vehicles Passive Safety Rating Method. Detroit.

Simpson, T. W. et al., 2004. Approximation Methods in Multidisciplinary Analysis and Optimization: A Panel Discussion. Structural and Multidisciplinary Optimization, 34(3), pp. 302-313.

TASS, n.d. www.tassinternational.com/madymo. [Online].

Vangi, D., 2008. Ricostruzione della dinamica degli incidenti stradali – principi e applicazioni. Florence: Firenze University Press.

Vangi, D., 2009. Energy loss in vehicle to vehicle oblique impact. Int. J. of Impact Engineering, 36(3), pp. 512-521.

vCRASH, A. I., n.d. www.vcrashusa.com. [Online].

Wei, Z., Karimi, H. R. & Robbersmyr, K. G., 2016. Analysis of the relationship between energy absorbing components and vehicle crash response, Tech. Rep. 2016-01-1541. SAE Technical Paper, Issue 2016-01-154.

Yildiz, A. R. & Solanki, K. N., 2012. Multi-objective optimization of vehicle crashworthiness using a new particle swarm based approach. Int. J. Adv. Manufact. Tech., 59(Issue 1–4), p. 367–376.